FATIGUE LIFE PREDICTION OF METALLIC MATERIALS USING THE TANAKA-MURA-WU MODEL

Siqi Li[1], Rong Liu[1], Xijia Wu[2] and Zhong Zhang[2]

[1] Department of Mechanical & Aerospace Engineering, Carleton University, Canada, siqili4@cmail.carleton.ca
[2] Structures and Materials Performance Laboratory, Institute for Aerospace Research, National Research Council Canada, Ottawa, Canada

Abstract: Computational fatigue design approach has achieved rapid advancement in recent years owing to its high efficiency and low cost. The Tanaka-Mura-Wu (TMW) model is one of the advanced approaches which considers fatigue crack nucleation to be caused by the accumulation of irreversible dislocation dipoles within the slip band and derives the fatigue crack nucleation life in terms of the dislocation pileup mechanism so that the model parameters only involve material physical properties such as elastic modulus, Poisson's ratio, surface energy and the Burger's vector. This article presents a study of the TMW model application to fatigue life predition for different engineering materials such as nickel-based alloy, low-carbon steel and alloy steel, hence to further validate the model by comparing the predicted fatigue lives with the Coffin-Manson-Basquin relation which is experimental-data-based, over the full fatigue range including low cycle fatigue (LCF) and high cycle fatigue (HCF). It is shown that the TMW model is able to provide class-A prediction for LCF without resorting to fatigue testing and with calibration at one stress level, it can be extended to the HCF regime. The model describes the full-range fatigue life in terms of material physical properties only, therefore it establishes a physics-based baseline for characterizing the effects of other influencing factors including microstructure and surface roughness on the fatigue life of a material, which contribute to the uncertainty in fatigue scatter.

Keywords: Tanaka-Mura-Wu (TMW) model, Coffin-Manson-Basquin relation, low cycle fatigue (LCF), high cycle fatigue (HCF), fatigue life prediction

INTRODUCTION

Fatigue failure is extremely harmful to the structural integrity of engineering components as fatigue crack nucleation is insidious and very difficult to predict. Therefore, it is crucial to evaluate the fatigue durability of candidate materials for engineering structures to minimize the risk of catastrophic failure. Commonly, engineers have to perform fatigue testing, either stress or strain-controlled, to determine the fatigue properties of a material and establish the relationship between fatigue life and loading parameters. Basquin [1] proposed a power-law relationship between the stress amplitude and fatigue life, Coffin [2] and Manson [3] established a power-law relationship between the plastic strain range and fatigue life. By combining the Coffin-Manson relation and the Basquin equation, a total strain versus life relation can be obtained, known as the Coffin-Manson-Basquin equation, which has been widely accepted by

the engineering community to characterize the fatigue performance of engineering materials. However, since it is in essence a purely empirical relation, large amounts of experimental data have to be generated through coupon testing, followed by regression analysis to obtain the empirical constants in the Basquin-Coffin and Manson equation. Although testing method is straightforward and applicable, it costs a great deal of time and money. In material and component design for any mechanical/structural system application, testing method prolongs the development cycle, especially when the tests have to be carried out at high temperatures. Also, fatigue test data are often scattering, therefore, a large number of coupons are required in order to obtain reliable results.

Due to above issues, the concept of computational fatigue design has been proposed and received an increasing interest in recent years. Many fatigue life prediction models were developed in the past, but most of them still rely on experimental calibration [4], none can provide class-A prediction (forecast before the event occurs). To this end, new models such as physics-based models are needed to provide a more effective characterization of fatigue life for durability design. Fatigue damage in essence is associated with plastic deformation as a result of dislocation interactions. Tanaka and Mura [5] proposed a theoretical model where fatigue crack nucleation is envisaged to be caused by the accumulation of irreversible dislocation dipoles within the slip band, but they evaluated the plastic strain by integration of displacement, which resulted in a problem in the strain unit. Recently, Wu [6] revised the true plastic strain expression of the Tanaka-Mura model and re-derived the fatigue crack nucleation life based on the same dislocation pileup mechanism, but in terms of the Burger's vector, elastic modulus, and surface energy [7], leading to a new model, known as the Tanaka-Mura-Wu (TMW) model. The validity of the TMW model has been conducted with low cycle fatigue (LCF) data on copper, titanium, tungsten, stainless steel 316, Waspaloy and MAR-M 509 [8-13]. By comparison with the experimental data, it is established that a surface roughness factor R_S exists, which takes the value of 1 for the electropolished (ideally smooth) surface and 1/3 for the machined surface. Thus, it is shown that the TMW model is promising to provide class-A prediction for LCF durability without prior calibration to fatigue test data, which has an advantage over other theoretical and empirical models.

In this research, the TMW model is utilized to predict the full-range fatigue lives, that is, from LCF to high cycle fatigue (HCF), of a nickel-based alloy Inconel 617, a low-carbon steel SAE 1020 and an alloy steel SAE 4340, in particular, an attempt is made to combine the Ramberg-Osgood equation and the TMW model to establish a physics-based baseline for the characterization of fatigue crack nucleation life as a function of the total strain range, since the total strain is a measurable quantity in structural design, testing and monitoring. For numerical convenience, the fatigue life predictions are compared with the Coffin-Manson-Basquin equation which represents the best fit of the experimental data of these common engineering materials. The sensitivity of the dependence of fatigue durability on material microstructure and properties is also discussed in order to understand their effects as the source of scattering, so as to narrow down the uncertainty qualification in future studies.

MATERIALS AND FATIGUE TEST DATA FITTING

In this study, three materials, Inconel 617, SAE 1020 and SAE 4340, are selected for fatigue life prediction using the TMW model, because they represent different groups of common engineering materials and are subjected to fatigue in service, also the empirical constants in the Coffin-Manson-Basquin equation are obtainable in literature for these materials.

The chemical compositions of the three materials are given in Table 1. Inconel 617 is a solid-solution, nickel-chromium-cobalt-molydenum alloy with an exceptional combination of high-temperature strength and oxidation resistance; it was hot rolled, followed by annealing [14]. SAE 1020 is a low-carbon steel; it was hardened by heating between 815°C and 871°C, followed by water quenching, and then it was tempered [15]. SAE 4340 is an alloy steel; it was heated at 830°C for half hour in salt, followed by water quenching, and then it was tempered at 430°C in salt with air cooling [16].

Table 1: Chemical compositions of studied materials.

Material	Element (wt.%)				
Inconel 617	Ni	Cr	Co	Mo	Fe, Mn, Si, etc.
	≥44.5	20-24	10-15	8-10	Bal.
SAE 1020	Fe	Mn	C	S	P
	99.08-99.53	0.3-0.6	0.17-0.23	≤0.05	≤0.04
SAE 4340	Fe	Ni	Mn	Cr	Mo, C, Si, etc.
	96	1.83	0.7	0.7-0.9	Bal.

The stress amplitude versus fatigue life relationship is often expressed by the Basquin equation [1]

$$\frac{\Delta\sigma}{2} = \sigma_f'(2N_f)^b \quad (1)$$

and the plastic strain amplitude versus fatigue life is given by the Coffin-Manson equation [2, 3]

$$\frac{\Delta\varepsilon_p}{2} = \varepsilon_f'(2N_f)^c \quad (2)$$

where N_f is fatigue life (cycles to failure), $\Delta\sigma$ is applied stress range, $\Delta\varepsilon_p$ is applied plastic strain range, σ_f' is fatigue strength coefficient, b is fatigue strength exponent, ε_f' is fatigue ductility coefficient and c is fatigue ductility exponent. These empirical constants σ_f', b, ε_f', and c are empirical constants which can be obtained by fitting experimental data. To express the full range of fatigue, Coffin-Manson and Basquin equations are often combined into the following equation [17]

$$\frac{\Delta\varepsilon}{2} = \frac{\Delta\sigma}{2E} + \frac{\Delta\varepsilon_p}{2} = \frac{\sigma_f'}{E}(2N_f)^b + \varepsilon_f'(2N_f)^c \quad (3)$$

where $\Delta\varepsilon$ is the total strain range, E is the Young's modulus. Then the total strain versus life relation can be derived, as illustrated in Figure 1.

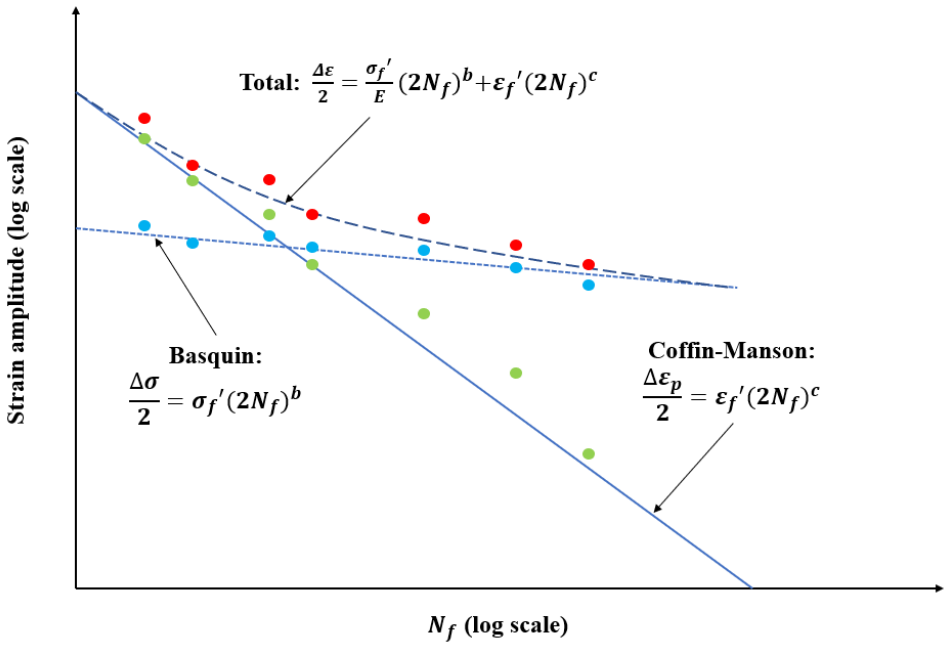

Figure 1: Total strain-life curve composed of Coffin-Manson and Basquin relations, each represents a linear regression of experimental data.

The fatigue properties such as the empirical constants σ_f', b, ε_f', and c in the Coffin-Manson-Basquin equation for Inconel 617, SAE 1020 and SAE 4340 were reported in literature [18-20], as presented in Table 2.

Table 2: Fatigue properties of studied materials.

Material	σ_f' (MPa)	b	ε_f'	c
Inconel 617	1519.55	-0.104	0.50	-0.57
SAE 1020	815	-0.110	0.25	-0.54
SAE 4340	1898	-0.090	0.67	-0.64

THE TMW MODEL PARAMETERS

Based on the dislocation pileup concept, the TMW model expresses the fatigue crack nucleation life in terms of plastic strain and stress ranges as [6, 7]

$$N_c = \frac{8(1-\nu)w_s}{\mu \boldsymbol{b}} \Delta\gamma^{-2} \tag{4}$$

$$N_c = \frac{2\mu w_s}{(1-\nu)\boldsymbol{b}} (\Delta\tau - 2k)^{-2} \tag{5}$$

where N_c is fatigue crack nucleation life, μ is shear modulus, w_s is surface energy, $\boldsymbol{b}$ is the Burger's vector, ν is Poisson's ratio, $\Delta\gamma$ is shear plastic strain range, $\Delta\tau$ is shear stress change, and k is lattice-friction stress, which corresponds to the critical resolved shear stress (CRSS) of active slip system.

To deal with real material coupons under uniaxial loading, the shear stress/strain range can be converted to normal stress/strain range, $\Delta\sigma$ and $\Delta\varepsilon_p$, following the Taylor relationship, $\sigma = \sqrt{3}\tau$ and $\gamma = \sqrt{3}\varepsilon_p$, and a surface roughness factor R_s is introduced to represent the effect of surface roughness condition such that Eqns. 4 and 5 turn into

$$N_c = \frac{8(1-\nu)R_s w_s}{3\mu \boldsymbol{b}} {\Delta\varepsilon_p}^{-2} \tag{6}$$

$$N_c = \frac{6\mu w_s}{(1-\nu)\boldsymbol{b}} (\Delta\sigma - 2\sigma_0)^{-2} \tag{7}$$

where $\sigma_0 = \sqrt{3}k$, which is the fatigue endurance limit for real material coupons. For crystalline materials, σ_0 is related to the critical resolved shear stress (CRSS), as demonstrated by the micro-pillar tests and molecular dynamics simulations [21, 22]. In pure metals, σ_0 arises from the Peierls-Nabarro resistance [23]. In complex alloys, it may be raised by various strengthening mechanisms including solid solution strengthening, precipitate strengthening and Hall-Petch relationship [7]. In this study, σ_0 is calibrated to the stress level at 10^7 cycles. Actually, it can be calibrated to any S-N curve point of the testing result in the HCF regime, better close to the fatigue endurance limit.

During fatigue, the cyclic stress - strain curve (CSSC) can be expressed by the Ramberg-Osgood equation [17]

$$\frac{\Delta\varepsilon}{2} = \frac{\Delta\sigma}{2E} + \frac{\Delta\varepsilon_p}{2} = \frac{\Delta\sigma}{2E} + \left(\frac{\Delta\sigma}{2K'}\right)^{1/n'} \tag{8}$$

where K' is plastic strength coefficient and n' is hardening exponent. Eqn. 8 is established connecting the peak points of the stabilized hysteresis loop (usually at the half-life point) without fracture. The cyclic hardening coefficients K' and n' can be determined by fitting experimental data. For Inconel 617, SAE 1020 and SAE 4340, the values of K' and n' are obtainable in literature [18-20], as presented in Table 3. The normal stress/strain range $\Delta\sigma$ and $\Delta\varepsilon_p$ for Eqns. 6 and 7 can be determined from Eqn. 8.

Table 3: Cyclic hardening coefficients of studied materials.

Material	K′ (MPa)	n′
Inconel 617	1910	0.12
SAE 1020	941	0.18
SAE 4340	1950	0.13

The TMW model employs only basic material physical properties such as the Burger's vector $\boldsymbol{b}$, shear modulus μ and surface energy w_s. The Burger's vector $\boldsymbol{b}$ is a character of slip systems in a given crystalline lattice structure, for instance, face centered cubic (fcc), body centered cubic (bcc) and hexagonal closely packed (hcp), etc. The shear modulus is related to the Young's modulus E by the relationship: $\mu = \frac{E}{2(1+\nu)}$ or it can be evaluated from the linear elastic behavior (as the slope of the initial stress - strain curve). The surface energy w_s is determined by [24]

$$w_s = w_s(T_m) + \phi(T)\frac{RT_m}{A} \tag{9}$$

where $w_s(T_m)$ is the surface energy at the melting temperature, A is the surface area per mole of surface atoms, $\phi(T)$ is a temperature-dependent parameter having a value ranging from 0 (at the melting point) to 1 (at the absolute zero-degree Kevin), and R is the universal gas constant. The values of $w_s(T_m)$ and $\frac{RT_m}{A}$ have been obtained for most metals [24]. It should be noted that the value of $\frac{RT_m}{A}$ is about one-tenth of $w_s(T_m)$ value for the same metal. Therefore, using the surface energy value at the absolute zero temperature or at the melting point is only about 10% in difference. For simplicity and consistency, in this study, it is assumed that $\phi(T)$ = 0.85 at room temperature (20℃).

Once the required material properties for the TMW model are determined, the material's fatigue life can be calculated straightforward using Eqn. 6 or Eqn. 7. While the determination of $\sigma_f{}'$, b, $\varepsilon_f{}'$, and c for the Coffin-Manson-Basquin equation has to be based on a large number of fatigue tests performed to failure, the shear modulus, Burger's vector and surface energy values can be easily found in materials handbooks or measured independently using physical methods. The values of the TMW model parameters for the studied materials are given in Table 4.

Table 4: The TMW model parameters of studied materials.

Material	ν	μ (GPa)	w_s (J/m^2)	σ_0 (MPa)	R_s	**b** (10^{-10} m)
Inconel 617	0.34	82.46	2.335	275	1/3	2.48
SAE 1020	0.29	79.45	2.373	100	1/3	2.48
SAE 4340	0.3	76.92	2.373	462	1/3	2.48

FATIGUE LIFE PREDICTION

LCF life prediction

In the LCF regime, the plastic strain is appreciable and the stress - strain response is controlled by the dislocation arrangements including veins, walls, labyrinth and cells. Apparently, such dislocation arrangements are more complicated than planar dislocation pile-ups as perceived by the TMW model. Nevertheless, the plastic strain life Eqn. 6 can still be valid by the equivalence of strain energy for crack nucleation, since the total input strain energy can always be divided into two parts: one part for increasing the microstructural entropy, and the rest will be released to form a crack.

The predicted fatigue lives of Inconel 617, SAE 1020 and SAE 4340 using Eqn. 6 are compared with the Coffin-Manson equation, as shown in Figure 2. Since the calculation of LCF life is independent of

fatigue testing, the prediction of Eqn. 6 is deemed to be a class-A prediction. It can be seen that for all the studied materials, the agreement between the Eqn. 6 prediction and the experimental behavior (the best-fit Coffin-Manson correlation) is within the typical fatigue scatter factor of 2. However, it should be noticed that with the plastic strain amplitude reducing, the relative error in determining the plastic strain from the total strain measurement becomes larger, and hence the Coffin-Manson correlation with the data in the LCF region involves measurement error. Because of this, variations in the slope of linear regression are often observed in experimental studies, even for the same material.

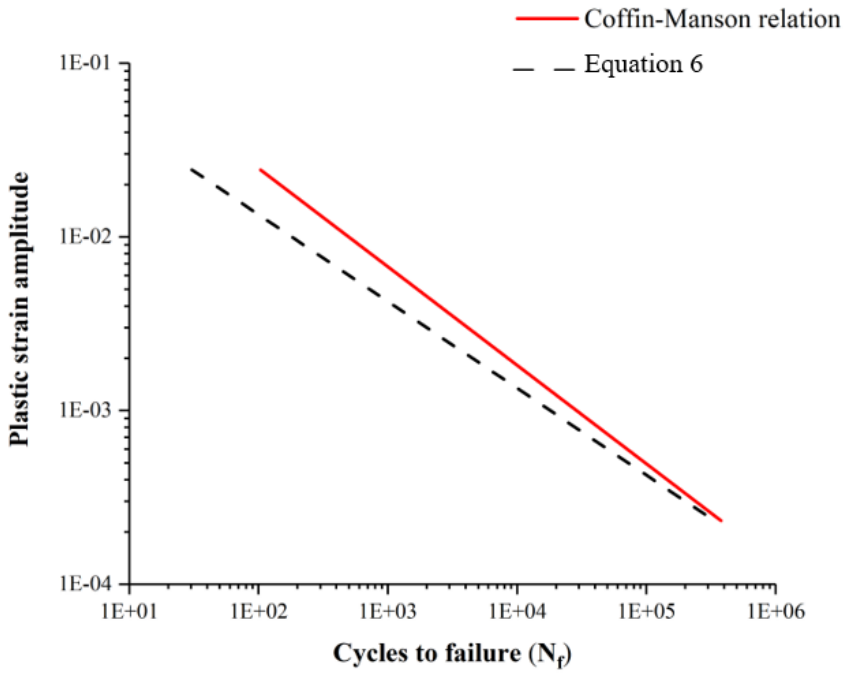

(a)

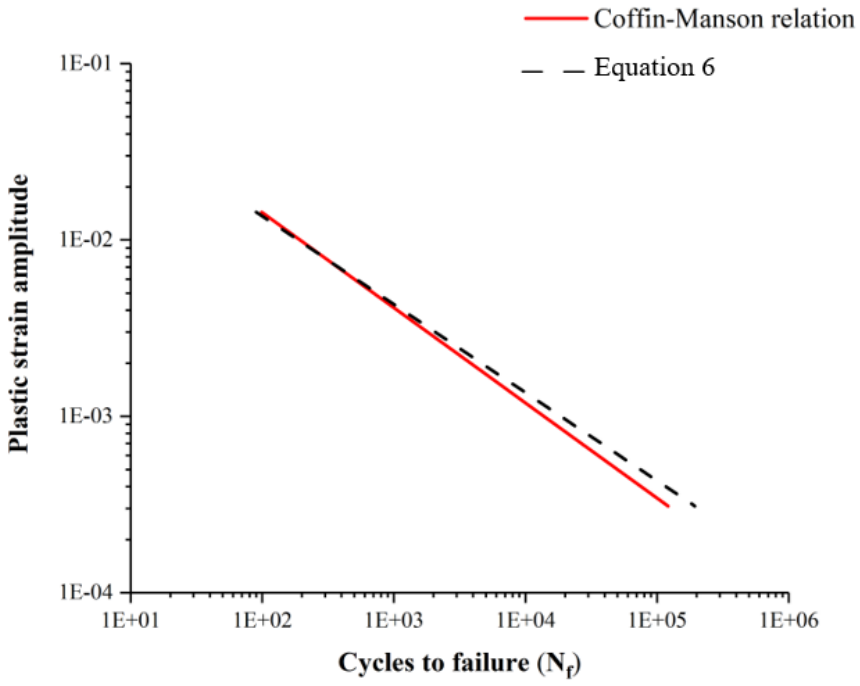

(b)

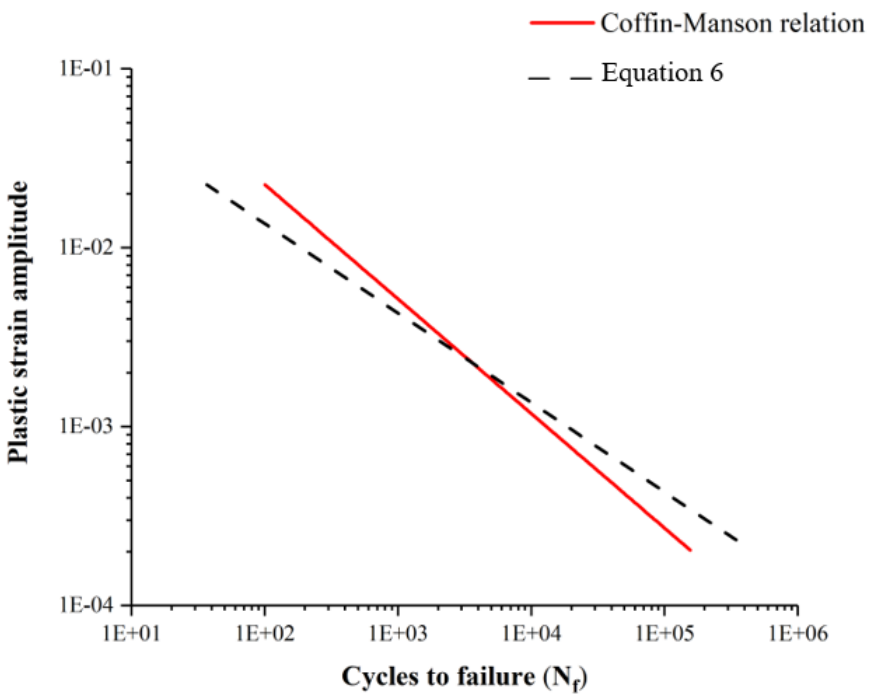

(c)

Figure 2: Comparison between predicted fatigue life with Eqn. 6 and the Coffin-Manson relation for (a) Inconel 617, (b) SAE 1020, (c) SAE 4340.

It is well known that the slope and intercept of linear regression in a log-log scale depend on the dataset (the number of tests and scatter). In its explicit form, Eqn. 6 does not cover the fatigue scatter. Therefore, the surface finish and microstructural factors appear to be hidden variables, since the microstructure is not uniform in a material and surface finish is not exactly the same by machining, particularly hand-polishing of coupons is often employed for laboratory testing. Nevertheless, Eqn. 6 appears to provide a physics-based baseline with which the effects of the aforementioned factors can be evaluated.

HCF life prediction

For HCF, the plastic strain is not macroscopically discernable, and the dislocation structure mainly consists of planar slip bands. A transmission electron microscopy (TEM) study has shown this to be true at low strain amplitudes [25]. The stress in the HCF regime can be accurately determined from the macroscopic elastic behavior of the material. Therefore, the stress-based Eqn. 7 is preferably used to assess the HCF behavior where the material response is predominantly elastic and the stress amplitude is a determinable load parameter. In this case, the microstructural slip resistance parameter σ_0 has to be calibrated to a known test result, as delineated above, σ_0 corresponds to the stress magnitude at the cycle of 10^7. The comparisons of the fatigue life predictions between Eqn. 7 and Eqn. 1 (the Basquin equation) for HCF below the yield strength of the studied materials are illustrated in Figure 3.

It is shown that the theoretical predictions from Eqn. 7 agree well with the Basquin curves in the HCF region ($N_f > 10^4$ cycles) with a typical scatter factor of 2 for most of the studied materials, except for SAE 1020. A note should be made here that the Basquin equation does not have a true fatigue endurance limit, therefore, the extrapolation of the Basquin equation fitted with the data at intermediate stress levels may be erroneous towards the low stress region. It is also generally recognized that the HCF behavior is very sensitive to the microstructure, typically with a scatter factor greater than 5. As the microstructural effect is not explicitly considered in the simple analytical equation, in-depth analysis is needed to describe the scatter for HCF.

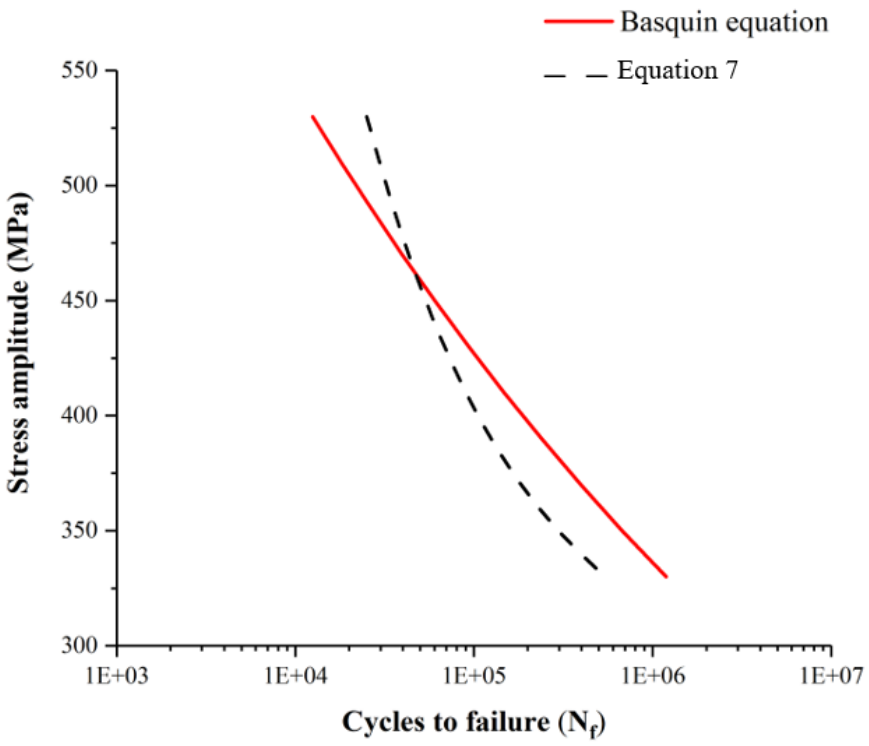
Basquin equation
Equation 7
Stress amplitude (MPa)
550
500
450
400
350
300
1E+03
1E+04
1E+05
1E+06
1E+07
Cycles to failure (N_f)

(a)

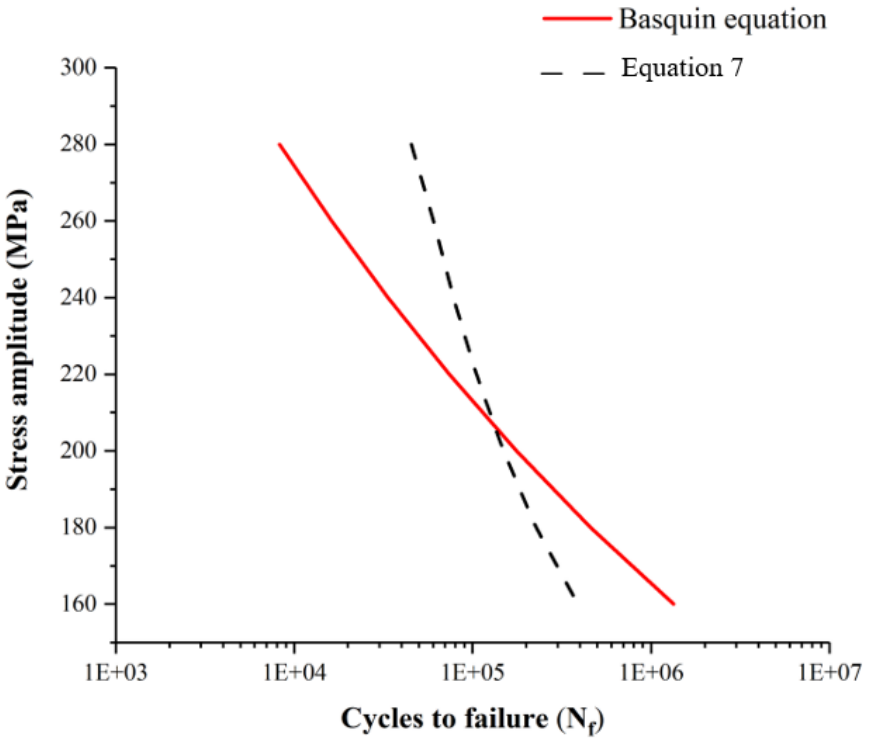
Basquin equation
Equation 7
Stress amplitude (MPa)
300
280
260
240
220
200
180
160
1E+03
1E+04
1E+05
1E+06
1E+07
Cycles to failure (N_f)

(b)

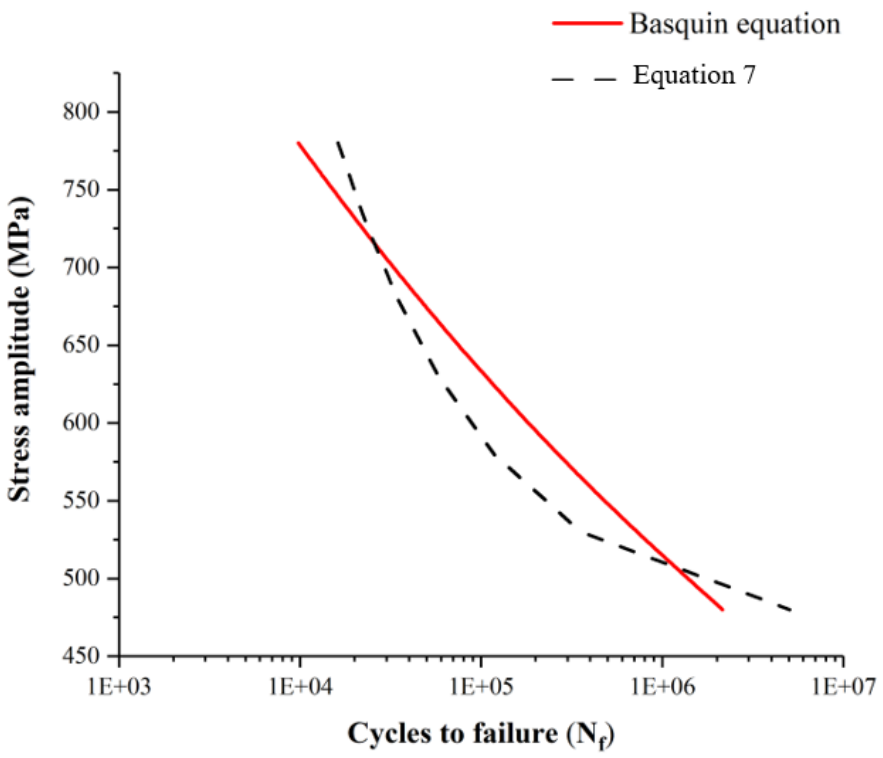

(c)

Figure 3: Comparison between predicted fatigue life with Eqn. 7 and the Basquin equation for (a) Inconel 617, (b) SAE 1020, (c) SAE 4340.

Full-range life prediction

For a real material, the cyclic stress - strain curve can be well-described by Eqn. 8 (the Ramberg-Osgood equation) [17]. In structural fatigue design, this stress - strain relationship is often used as the constitutive law for stress analysis using finite element method (FEM). Therefore, it is important to predict fatigue life based on the total strain in engineering design and health monitoring of engineering structures and components, because only the total strain can be directly measured by strain gauges or sensors when conducting a component/structural fatigue test and when it is being monitored during service. Once the total strain is determined/measured, the stress and plastic strain can be determined from the Ramberg-Osgood equation (Eqn. 8).

The fatigue life predictions as a function of the total strain for the studied materials using the TMW model are presented in Figure 4 in comparison with the Coffin-Manson-Basquin equation. For the argument sake, a scatter factor of 2 is uniformly applied to the experimental curve, as covered by a grey band. The overall validity of the TMW model is thus demonstrated since the predictions mostly fall in the scatter band, in particular, when the fatigue life $N_f < 10^4$. As shown in Figure 1, traditionally, the total strain versus life relationship is perceived to be the result of the superposition of a plastic component and an elastic component, both parts have to be established by regression of the experimental data without physical explanation. The TMW model describes the LCF and HCF regimes based on the same mechanism — dislocation dipole pileup.

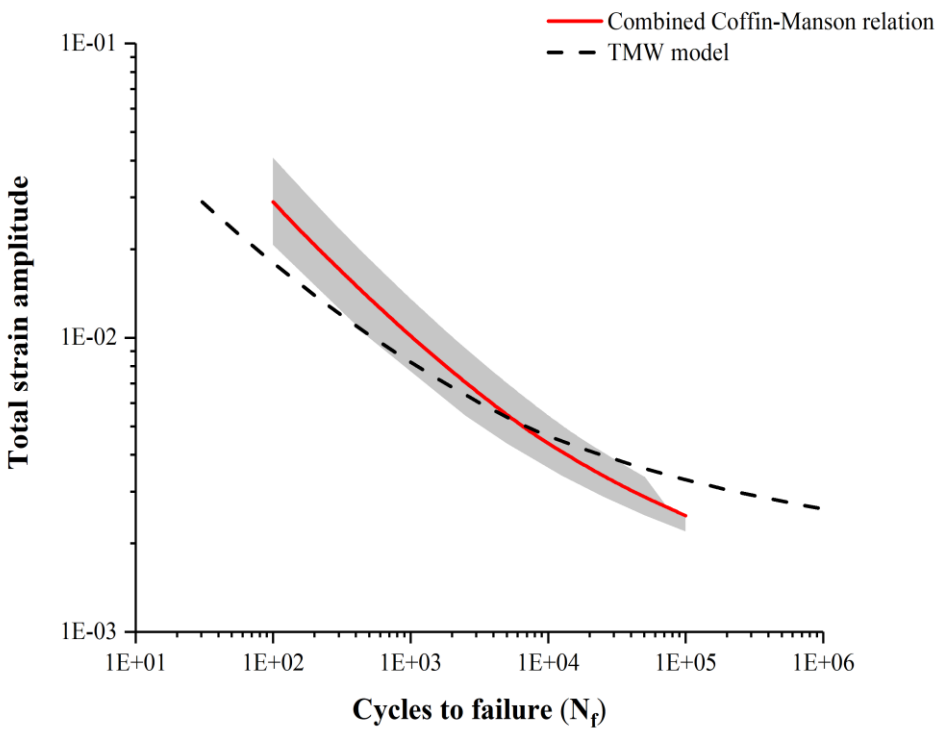
Combined Coffin-Manson relation
TMW model
Total strain amplitude
1E-01
1E-02
1E-03
1E+01
1E+02
1E+03
1E+04
1E+05
1E+06
Cycles to failure (N_f)

(a)

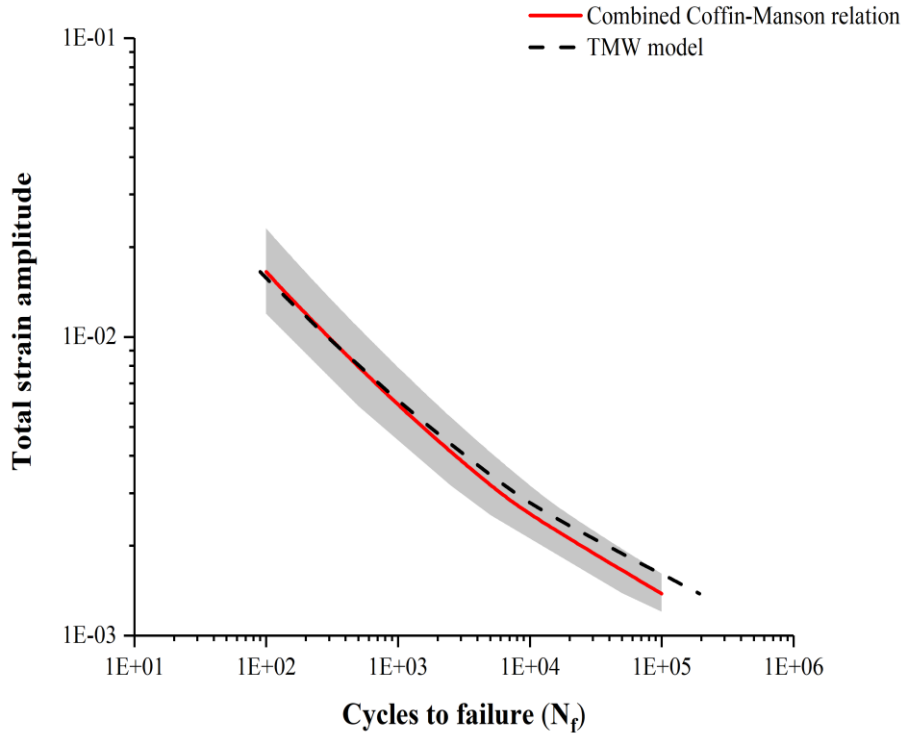
Combined Coffin-Manson relation
TMW model
Total strain amplitude
1E-01
1E-02
1E-03
1E+01
1E+02
1E+03
1E+04
1E+05
1E+06
Cycles to failure (N_f)

(b)

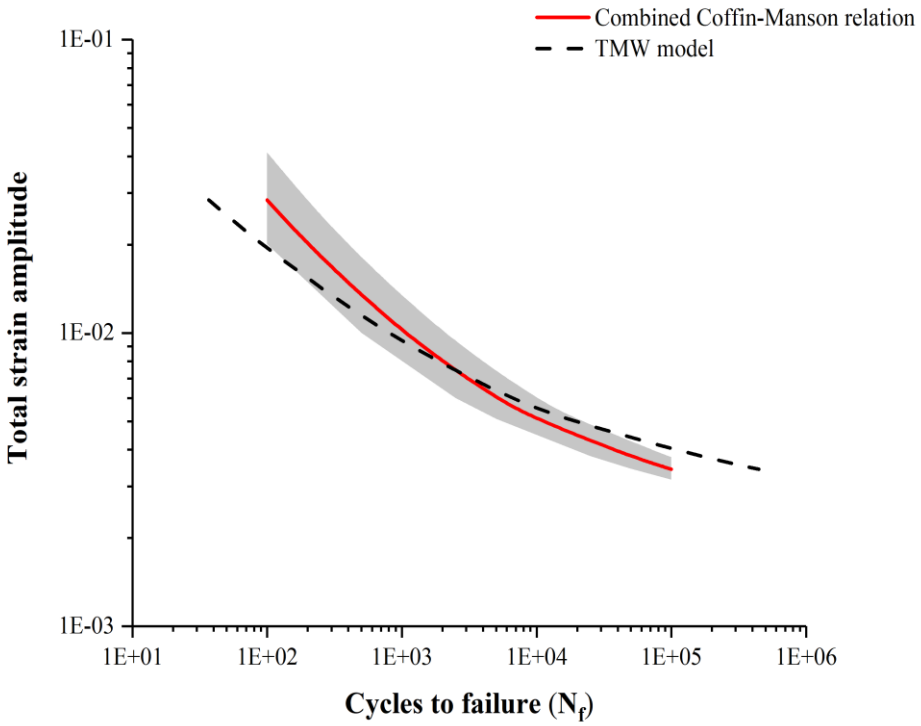

(c)

Figure 4: Comparison of fatigue life prediction between the TMW model and Eqn. 3 for (a) Inconel 617, (b) SAE 1020, (c) SAE 4340.

Discussion

It is seen that the disparity of Eqn. 7 (the stress-based equation) with Eqn. 1 (the Basquin equation) becomes increasingly large towards the fatigue limit. This can be attributed to two reasons. One is that the Basquin equation does not have a fatigue limit so that its representation of the material behavior which does exhibit a fatigue limit is questionable. The other is that the fatigue life near the fatigue limit is very sensitive to the material microstructure (often with an experimental scatter factor > 5), which cannot be fully taken into account by the analytical model. The basic material properties such as shear modulus μ, Poisson's ratio ν, surface energy w_s and the Burger's vector $\boldsymbol{b}$ do not cause very much uncertainty, because they can be accurately determined by physical testing with errors less than 5%. On the other hand, microstructural variations can strongly influence σ_0. A sensitivity function can be defined regarding σ_0 as

$$S(N_f, \sigma_o) \stackrel{\text{def}}{=} \frac{\sigma_0}{N_f}\frac{\partial N_f}{\partial \sigma_0} = \frac{4\sigma_0}{\Delta\sigma - 2\sigma_0} \tag{10}$$

It can be inferred from Eqn. 10 that when the stress amplitude is close to σ_0, the relative error in fatigue life can be orders-of-magnitude larger than at intermediate stress levels.

Another uncertainty factor lies in the surface roughness factor R_s, which can be a function of the arithmetic roughness R_a. Since it is a linear proportional factor, the relative error in the life prediction with regards to the surface roughness effect is a constant. In this study, an average value of 1/3 for the surface roughness factor $R_s$is applied to all materials in nominally machined conditions under LCF conditions. Precise characterization would need detailed information on surface finishing, but it is statistical by nature. In addition to surface finish, other manufacturing defects such as inclusions and porosity may also exist in real materials, which are all known to affect the fatigue resistance of materials. Therefore, future studies are needed to focus on determining σ_0 and R_s as well as microstructural crack nucleation at the sites with reduced surface energy. For example, the grain boundary surface energy is

usually half of the free surface energy. In this sense, the TMW model can indeed be improved with considerations of microstructure effects for fatigue design.

CONCLUSIONS

1. The TMW model is derived from the mechanism of dislocation dipole pileup, which is delineated by material physical properties such as elastic modulus, Poisson's ratio, surface energy and the Burger's vector

2. The TMW model is presented with a plastic strain-based expression and a stress-based expression for fatigue crack nucleation. The plastic strain-based equation can provide a class-A prediction for the LCF life and the stress-based equation is more suitable for HCF life prediction where macroscopic plasticity is discernible, but the lattice resistance σ_0 needs to be calibrated to one S-N curve point close to the fatigue endurance limit.

3. The TMW is shown to be applicable to nickel-based alloy, low-carbon steel and alloy steel within a scatter factor of 2 as compared with the Coffin-Manson-Basquin relation. By virtue of the physics of failure, it offers a greater applicability for crystalline materials.

4. In a combined use with the Ramberg-Osgood equation, the TMW model can be used to establish the relationship between fatigue life and total strain over the full range including LCF and HCF, which is more useful in structural fatigue analysis and monitoring.

5. The TMW model provides a physics-based baseline of fatigue analysis. The sensitivity of the TMW model is shown to be mostly influenced by the lattice resistance σ_o and roughness factor R_s. Therefore, future research should be focused on these issues to narrow down the uncertainty quantification.

REFERENCES

[1] Basquin, O.H. (1910), *Amer. Soc. Test. Mater. Proceed.*, vol. 10, p. 625.
[2] Coffin, L.F. (1954), *Trans. Amer. Soc. Mech. Eng.*, vol. 76, p. 931.
[3] Manson, S.S. (1954), *NASA Report*, vol. 1170, p. 9
[4] Santecchia, E. and hamouda, A.M.S. (2016), *Advan. Mater. Sci. Eng.*, vol. 2016, p. 1.
[5] Tanaka, K. and Mura, T. (1981), *J. Appl. Mech.*, vol. 48, n. 1, p. 97.
[6] Wu, X.J. (2018), *Fatigue Fract. Eng. Mater. Struct.*, vol. 41, n. 4, p. 894.
[7] Wu, X.J. (2019), *Deformation and Evolution of Life in Crystalline Materials*, CRC Press, Boca Raton.
[8] Reuchet, J. and Remy, L. (1979), *Fatigue Fract. Eng. Mater. Struct.*, vol. 2, n. 1, p. 51.
[9] Zhang, Z.F., Gu, H.C. and Tan, X.L. (1998), *Mater. Sci. Eng. A*, vol. 252, n. 1, p. 85.
[10] Wareing, J. and Vaughan, H.G. (1979), *Met. Sci.*, vol. 13, n. 1, p. 1.
[11] Reuchet, J. and Remy, L. (1983), *Mater. Sci. Eng.*, vol. 58, n. 1, p. 33.
[12] Bradley, A.L., Jayaraman, N. and Stephen, D.A. (1984), *Mater. Sci. Eng.*, vol. 66, n. 2, p. 151.
[13] Schmunk, R.E. and Korth, G.E. (1981), *J. Nucl. Mater.*, vol. 104, p. 943.
[14] ASTM International (2008), *Standard Specification for Nickel-Chromium-Iron Alloys*, ASTM International, West Conshohocken.
[15] SAE International (1982), *SAE J1099 Technical Report on Fatigue Properties, SAE Handbook*, SAE International, USA.
[16] Conle, F.A., Landgraf, R.W. and Richards, F.D. (1984), *Materials Data Book: Monotonic and Cyclic Properties of Engineering Materials*, Ford Motor Company, Scientific Research Staff, Dearborn.
[17] Stephens, R.I., Fatemi, A., Stephens, R.R. and Fuchs, H.O. (2001), *Metal Fatigue in Engineering*, 2nd Eedition, John Wiley & Sons, Inc, New York.

[18] Kim, S.J., Dewa, R.T., Kim, W.G. and Kim, M.H. (2015), *Advan. Mater. Sci. Eng.*, vol. 2015, p. 207497.
[19] Wu, S.C., Xu, Z.W., Yu, C., Kafka, O.L. and Liu, W.K. (2017), *Inter. J. Fatigue*, vol. 103, p. 185.
[20] Brennan, F.P. (1994), *Inter. J. Fatigue*, vol. 16, n. 5, p. 351.
[21] Mlikota, M. and Schmauder, S. (2018), *Metals*, vol. 8, n. 11, p. 883.
[22] Mlikota, M. and Schmauder, S. (2020), *Metals*, vol. 10, n. 6, p. 803.
[23] Ali, A. (2007), *Strengthening Mechanisms in Crystal Plasticity*, Oxford University Press, Oxford.
[24] Tyson, W.R. and Miller, W.A. (1977), *Surf. Sci.*, vol. 62, p. 267.
[25] Kaiju, L., Ankur, C., Aditya, S.T., Jens, F., Alexander, K., Martin, H. and Jarir, A. (2021), *Acta Materialia*, vol. 215, p. 117089.